IEEE Access
Multidisciplinary ⋮ Rapid Review ⋮ Open Access Journal

Received 11 January 2023, accepted 11 February 2023, date of publication 16 February 2023, date of current version 23 February 2023.
Digital Object Identifier 10.1109/ACCESS.2023.3246397

RESEARCH ARTICLE

UTD-PO Solution for E-Plane Radiation Pattern Calculation of Rectangular Horn Antennas With Rectangular-Shaped Corrugations

JOSÉ LORENTE-LÓPEZ[1], JOSÉ-VÍCTOR RODRÍGUEZ[2], FERNANDO QUESADA-PEREIRA[2], (Member, IEEE), LEANDRO JUAN-LLÁCER[2], (Senior Member, IEEE), AND IGNACIO-RODRÍGUEZ-RODRÍGUEZ[3]
[1]Departamento de Ciencias de la Computación, Universidad de Alcalá, Alcalá de Henares, 28802 Madrid, Spain
[2]Departamento de Tecnologías de la Información y las Comunicaciones, Universidad Politécnica de Cartagena, Antiguo Cuartel de Antigones, Cartagena, 30202 Murcia, Spain
[3]BioSIP Group, Departamento de Ingeniería de Comunicaciones, Universidad de Málaga, 29071 Málaga, Spain

Corresponding author: José Víctor Rodríguez (jvictor.rodriguez@upct.es)

This work was supported in part by the Ministerio de Ciencia e Innovación, Spain, through projects PID2019-107885GB-C33 and PID2019-103982RB - MCIN/AEI/10.13039/501100011033 (the latter is the Subproject C42 Coordinated Research and Development Project); and in part by the Fundación Séneca, Agencia de Ciencia y Tecnología de la Región de Murcia, Spain, under project 22076/PI/22, which is included in the Regional Program for the Promotion of the Research (2022) of the Fundación Séneca-Agencia de Ciencia y Tecnología de la Región de Murcia (Componentes radiantes y de filtrado de microondas para satélites emergentes).

ABSTRACT Proposing a novel hybrid uniform theory of diffraction-physical optics (UTD-PO) formulation, we develop a method to calculate the E-plane radiation pattern of corrugated E-plane rectangular horn antennas with rectangular corrugations. We derive the technique from the estimation of the total field that reaches the emitting source (a magnetic current line), thereby assuming the impingement of a plane wave above the horn (reciprocity is applied). To validate our method, we compare the performance of the UTD-PO analysis with that of the electric field integral equation (EFIE) solved using the method of moments (MoM). Our method shows improved computational efficiency over EFIE and other numerical techniques that fully discretize the geometry.

INDEX TERMS Corrugated antennas, pattern analysis, multiple-diffraction, uniform theory of diffraction.

I. INTRODUCTION

Corrugated horn antennas with rectangular corrugations have distinct features that set them apart from conventional (i.e., non-corrugated) horns. As such, they are well-suited for application at microwave frequencies, e.g., when there is a need for a low cross-polar response, radiation pattern symmetry, low side-lobes and back-lobes, or broad-band performance [1], [2], [3], [4], [5], [6], [7], [8], [9], [10]. However, analyzing the radiation patterns of corrugated horns in or below the mm-band (encompassing a number of corrugations per wavelength) demands complex numerical techniques that engender high computational costs [11], [12].

Meanwhile, as shown in [13] and [14], for non-corrugated E-plane rectangular horns the E-plane radiation pattern can be investigated via the ray-based uniform theory of diffraction (UTD). This method uses the calculation of the total field arriving at the emitting source (a magnetic current line), assuming the impingement of a plane wave above the horn (reciprocity is applied). Notably, such a rectangular horn's E-plane radiation pattern can be estimated via a 2-D approach as the illumination remains constant [13].

This approach has produced applicable hybrid UTD-physical optics (PO) solutions for corrugated horn antennas whose corrugations are either V-shaped [14] or cylindrical [15]. Such methods demonstrate enhanced computational efficiency compared to alternative numerical techniques that fully segment the geometry.

In light of this, the current work proposes a hybrid UTD-PO formulation that offers an easier and faster way to estimate the E-plane radiation patterns of corrugated

The associate editor coordinating the review of this manuscript and approving it for publication was Mehmet Alper Uslu.

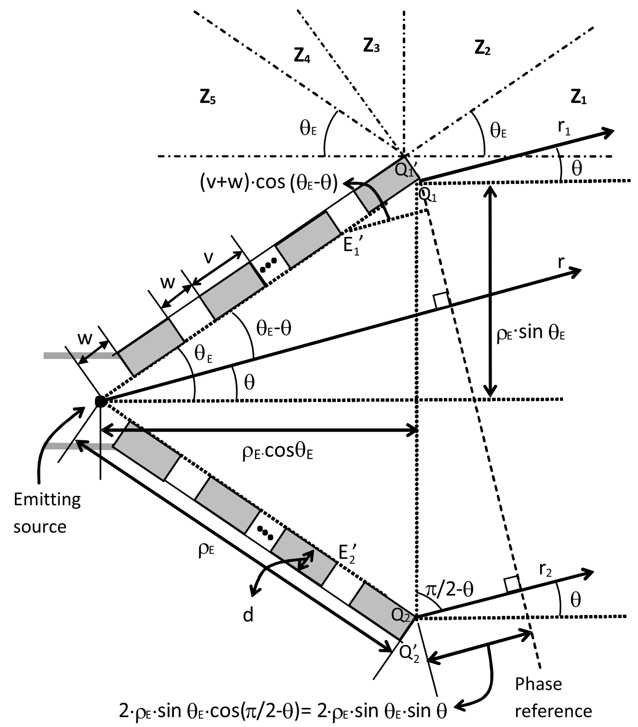

FIGURE 1. **Schema of the investigated E-plane of a corrugated E-plane rectangular horn antenna.**

E-plane rectangular horn antennas that have typically used rectangular-shaped corrugations, i.e., are spaced and distributed equally across the horn's faces. The presented technique is eminently applicable for investigating very densely corrugated horn antennas with numerous corrugations per wavelength.

II. THEORETICAL FORMULATIONS

Based on the UTD-PO solutions for evaluating multiple radio wave diffraction over a series of plateaus, as given in [16] and [17] for positive and negative incidence, respectively, we may determine the normalized E-plane radiation pattern of an E-plane rectangular horn with n rectangular corrugations (see Fig.1 for the E-plane schema) by calculating the following:

$$Pattern(dB) = 20\log_{10}\left(\frac{|E_T(\theta)|}{|E_T(\theta=0)|}\right) \tag{1}$$

where $E_T(\theta)$ is the total field arriving at the emitting source (considering reciprocity).

As Fig. 1 shows, we assume that this horn has n conducting rectangular corrugations of width v and height d that are distributed and spaced at a constant distance w along the horn's arms; w is also assumed to separate the emitting source from the preceding rectangular section. Additionally, ρ_E is the length of the faces of the horn and θ_E is the half-angle of the aperture of the horn.

Fig. 1 presents three basic possible field contributions, namely the direct ray (r), the ray multiply diffracted at the horn's upper face (r_1), and the ray multiply diffracted at the horn's lower face (r_2). Hence, five different zones can be distinguished (Z_{1-5}), in line with the contributions that reach the receiving point at a given θ between 0 and π; hence, $E_T(\theta)$ takes on a different expression in assocation with the considered zone:

$\mathbf{Z_1}$ ($\theta \leq \theta_E$):

$$E_T(\theta) = E_{r+r_1}(\theta) + E_{r_2}(\theta) \tag{2}$$

with

$$\begin{aligned}
&E_{r+r_1}\\
&= \frac{1}{2n}\left\{\sum_{q=0}^{n-1} E_q\left[\exp\left[-jk(n-q)(v+w)\cos\left(\theta_E-\theta\right)\right]\right.\right.\\
&\quad + \frac{1}{\sqrt{(n-q)(v+w)}}\\
&\quad \cdot D\left(\phi' = \frac{\pi}{2} + (\theta_E-\theta), \phi = \frac{3\pi}{2}, L = (n-q)(v+w)\right)\\
&\quad \left.\times \exp\left[-jk(n-q)(v+w)\right]\right]\\
&\quad + \sum_{r=1}^{n} E(r)\left[\exp\left[-jk\left[(n-r)(v+w)+w\right]\cos\left(\theta_E-\theta\right)\right]\right.\\
&\quad + \frac{1}{\sqrt{(n-r)(v+w)+w}}\\
&\quad \cdot D\left(\phi' = (\theta_E-\theta), \phi = \pi, L = (n-r)(v+w)+w\right)\\
&\quad \left.\left.\times \exp\left[-jk\left[(n-r)(v+w)+w\right]\right]\right]\right\}.
\end{aligned} \tag{3}$$

This term represents the field of the r and r_1 contributions (using the solution presented in [16] for positive incidence). E_0 is the incident plane wave's relative amplitude, k is the free-space wave number, and $D(\phi, \phi, L)$ is the diffraction coefficient for a conducting wedge as per [18]; also

$$\begin{aligned}
&E(r)\\
&= \frac{1}{2n-1}\left\{\sum_{m=0}^{n-1} E_m\left[\exp\left[-jk\left[(n-m)(v+w)-w\right]\right.\right.\right.\\
&\quad \left.\cos\left(\theta_E-\theta\right)\right] + \frac{1}{\sqrt{(n-m)(v+w)-w}}\\
&\quad \cdot D\left(\phi' = \frac{\pi}{2} + (\theta_E-\theta), \phi = \frac{3\pi}{2},\right.\\
&\quad \left.\left. L = (n-m)(v+w)-w\right) \exp\left[-jk\left[(n-m)(v+w)-w\right]\right]\right]\\
&\quad + \sum_{p=1}^{n-1} E(p)\left[\exp\left[-jk(n-p)(v+w)\cos\left(\theta_E-\theta\right)\right]\right.\\
&\quad + \frac{1}{\sqrt{(n-p)(v+w)}}\\
&\quad \cdot D\left(\phi' = (\theta_E-\theta), \phi = \pi, L = (n-p)(v+w)\right)\\
&\quad \left.\left.\exp\left[-jk(n-p)(v+w)\right]\right]\right\}
\end{aligned} \tag{4}$$

Meanwhile, based on the solution suggested by [17] for negative incidence over a series of plateaus, we can estimate the second term of (2), $E_{r2}(\theta)$, as

$$E_{r_2} = \frac{1}{n'+1}\sum_{m=0}^{n'-1} E_{n'm} \tag{5}$$

where

$$E_{n'm} = E'_{n'm} \pm \left(E''_{n'm} - E'''_{n'm}\right) \tag{6}$$

with (7)–(9), as shown at the bottom of the page, being that

$$E\,(1) = E_0\frac{1}{\sqrt{v}}\cdot D\left(\phi' = \frac{\pi}{2}, \phi = \frac{3\pi}{2}, L = v\right)\exp\left(-jkv\right) \tag{10}$$

$$\begin{aligned} E'\,(1) = E_0\Bigg[&\exp\left(-jkv\right) + \frac{1}{\sqrt{v}} \\ &\cdot D\left(\phi' = \frac{\pi}{2}, \phi = \frac{3\pi}{2}, L = v\right)\exp\left(-jkv\right)\Bigg] \end{aligned} \tag{11}$$

$$w' = (n-m)\,w + (n-m-1)\,v \tag{12}$$

$$n' = n-1, \tag{13}$$

assuming Q_2 and Q'_2 are the same point, and

$$\begin{aligned} E(0) &= E'_2 \\ &= \frac{E_0}{2\cdot\sqrt{L_2}}D(\phi'_2, \phi_2, L_2) \\ &\quad\times\exp\left[-jk\left(w + 2\cdot\rho_E\sin\theta_E\cdot\sin\theta\right)\right] \end{aligned} \tag{14}$$

where $D(\phi_2, \phi'_2, L_2)$ is the diffraction coefficient for an edge, as per [19]; also

$$L_2 = w \tag{15}$$

$$\phi_2 = 2\pi \tag{16}$$

$$\phi'_2 = \pi + \theta_E + \theta \tag{17}$$

$$E_i = \begin{cases} E(0), & if\ m = 0 \\ E_m & if\ m \neq 0 \end{cases} \tag{18}$$

Here, to calculate E_{r2}, we consider the first diffraction at the edge of the end of the horn's lower arm (Q_2 and Q'_2 are assumed to be co-located, as with a non-corrugated horn), which delineates the field over the subsequent rectangle (E'_2). With the direct ray having already been considered in (3), we then calculate the remaining multiple-rectangle diffraction via the grazing incidence over the rectangular sections; hereby, the smaller angle of incidence ($\theta_E - -\theta$) elevates the relevance of the multiple diffraction effect compared to that due to the array of corrugations at the horn's lower arm, which has a greater angle of incidence ($\theta_E + \theta$).

Z_2 ($\theta_E < \theta \leq \pi/2$):

$$E_T(\theta) = E_{r_1}(\theta) + E_{r_2}(\theta) \tag{19}$$

with

$$E_n = \frac{1}{n}\sum_{m=0}^{n-1} E_{nm} \tag{20}$$

considering (6), and (21)–(23), as shown at the bottom of the next page, considering (12), and

$$E_i = \begin{cases} 1, & if\ m = 0 \\ E_m & if\ m \neq 0 \end{cases} \tag{24}$$

$$\begin{aligned} E\,(1) = E_0\frac{1}{\sqrt{v}}\cdot D\left(\phi' = \frac{\pi}{2} + \alpha, \phi = \frac{3\pi}{2}, L = v\right) \\ \times\exp\left(-jkv\right) \end{aligned} \tag{25}$$

$$\begin{aligned} E'\,(1) = E_0\Bigg[&\exp\left(-jkv\cos\alpha\right) + \frac{1}{\sqrt{v}} \\ &\cdot D\left(\phi' = \frac{\pi}{2} + \alpha, \phi = \frac{3\pi}{2}, L = v\right)\exp\left(-jkv\right)\Bigg], \end{aligned} \tag{26}$$

with $\alpha = \theta_E - \theta$.

Furthermore, the second term of (19), $E_{r2}(\theta)$, can be calculated as in Z_1.

Z_3 ($\pi/2 < \theta \leq \theta_E + \pi/2$):

$$E_T(\theta) = E_{r_1}(\theta), \tag{27}$$

$$E'_{n'm} = \frac{1}{2}\left[\begin{aligned} &E_i\frac{1}{\sqrt{(v+w')}}D\left(\phi' = \frac{\pi}{2}, \phi = \frac{3\pi}{2}, L = \left(v+w'\right)\right)\exp\left(-jk\left(v+w'\right)\right) \\ &+E\,(1)\frac{1}{\sqrt{w'}}D\left(\phi' = \frac{\pi}{2}, \phi = \frac{3\pi}{2}, L = w'\right)\exp\left(-jkw'\right) \end{aligned}\right] \tag{7}$$

$$E''_{n'm} = E_i\left(\begin{aligned} &\exp\left(-jk\left(v+w'\right)\right) + \exp\left(-jkv\right)\frac{1}{\sqrt{w'}} \\ &\cdot D\left(\phi' = \frac{\pi}{2}, \phi = \frac{3\pi}{2}, L = w'\right)\exp\left(-jkw'\right) \end{aligned}\right) \tag{8}$$

$$E'''_{n'm} = \frac{1}{2}\left[\begin{aligned} &E_i(\exp\left(-jk\left(v+w'\right)\right) + \frac{1}{\sqrt{v+w'}} \\ &\cdot D\left(\phi' = \frac{\pi}{2}, \phi = \frac{3\pi}{2}, L = \left(v+w'\right)\right)\exp\left(-jk\left(v+w'\right)\right)) \\ &+E'\,(1)\left[\exp\left(-jkw'\right) + \frac{1}{\sqrt{w'}}\cdot D\left(\phi' = \frac{\pi}{2}, \phi = \frac{3\pi}{2}, L = w'\right)\exp\left(-jkw'\right)\right] \end{aligned}\right] \tag{9}$$

where $E_{r1}(\theta)$ can be calculated as in Z_2.

$$Z_4(\theta_E+\pi/2<\theta\leq\pi-\theta_E):$$

Consider (27), with

$$E_{r_1}=\frac{1}{n'+1}\sum_{m=0}^{n'-1}E_{n'm} \tag{28}$$

and expressions (6)-(13), with Q_1 and Q_1' now being assumed to be co-located, and

$$E(0)=E_1'=\frac{E_0}{2\cdot\sqrt{L_1}}D(\phi_1',\phi_1,L_1)\exp[-jkw] \tag{29}$$

with $D(\boldsymbol{\phi_1},\boldsymbol{\phi_1'},\boldsymbol{L_1})$ once more being the diffraction coefficient for an edge, as per [19], and

$$L_1=w \tag{30}$$
$$\phi_1=0 \tag{31}$$
$$\phi_1'=\pi-\theta_E+\theta, \tag{32}$$

with also considering (18).

Hereby, we obtain E_{r1} in the same manner with which E_{r2} was estimated in Z_1.

$\mathbf{Z_5}$ (π-$\theta_E<\theta\leq\pi$):

Consider (19), with the estimation of E_{r1} being as in Z_4 and that of E_{r2} as in Z_1, except that here,

$$\phi_2'=\theta_E-\pi+\theta \tag{33}$$

III. RESULTS

As clarified in Section II, Fig. 2 presents a corrugated E-plane rectangular horn's E-plane radiation pattern as estimated using the proposed UTD-PO technique, assuming $\rho_E=15\lambda$, $\theta_E=35°$, 40 rectangular corrugations, vertical/hard polarization, $v=0.26\lambda$, and $d=0.375\lambda$.

To validate the presented UTD-PO solution, we performed a comparison between this pattern and the pattern obtained for the same structure and parameters but based on [12]'s solution, which applies a standard two-dimensional electric field integral equation (EFIE) that is solved using the method of moments (MoM) (through a code programmed by the authors in FORTRAN 90). Based on subsectional, triangular-shaped basis functions with linear variation defined in two adjacent mesh segments, it was possible to calculate the integral equation via the expansion of the unknown electric current density; this was tested using these functions via a Galerkin approach. To be more specific, 1531 basis functions were used to produce the simulation of the corrugated horn with rectangular corrugations in Fig. 2, thereby making sure that there was at least one basis function every 0.2λ; the evaluation of the reaction integrals was performed with the maximum fifth order Gauss-Legendre quadrature rule. We checked the numerical convergence of the integral equation technique by progressively increasing the number of basis functions and mesh segments. The numerical convergence was achieved for a mesh segment length below

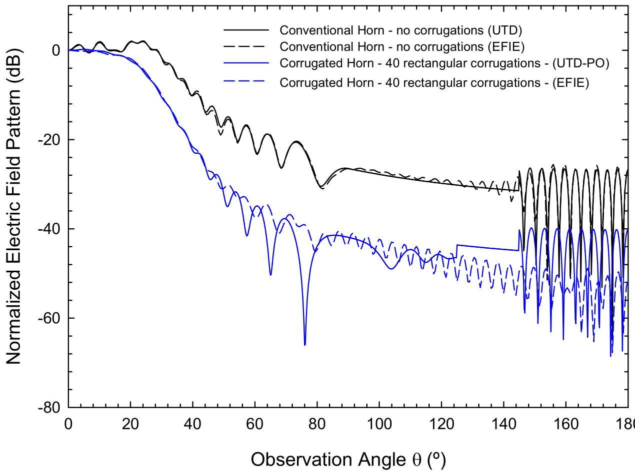

FIGURE 2. E-plane radiation patterns of a corrugated horn with 40 rectangular corrugations – comparing the UTD-PO approach proposed here with the EFIE technique [12]. The plot also presents the E-plane radiation pattern of an equivalent horn with no corrugations. $\rho_E=15\ \lambda$, $v=0.26\lambda$, $d=0.375\lambda$, and $\theta_E=35°$.

$$E_{nm}'=\frac{1}{2}\left[\begin{array}{l}E_i\frac{1}{\sqrt{(v+w')}}D\left(\phi'=\frac{\pi}{2}+\alpha,\phi=\frac{3\pi}{2},L=(v+w')\right)\exp\left(-jk\left(v+w'\right)\right)\\+E\left(1\right)\frac{1}{\sqrt{w'}}D\left(\phi'=\frac{\pi}{2}+\alpha,\phi=\frac{3\pi}{2},L=w'\right)\exp\left(-jkw'\right)\end{array}\right] \tag{21}$$

$$E_{nm}''=E_i\left(\begin{array}{l}\exp\left(-jk\left(v+w'\right)\cos\alpha\right)+\exp\left(-jkv\cos\alpha\right)\frac{1}{\sqrt{w'}}\\\cdot D\left(\phi'=\frac{\pi}{2}+\alpha,\phi=\frac{3\pi}{2},L=w'\right)\exp\left(-jkw'\right)\end{array}\right) \tag{22}$$

$$E_{nm}'''=\frac{1}{2}\left[\begin{array}{l}E_i(\exp\left(-jk\left(v+w'\right)\cos\alpha\right)+\frac{1}{\sqrt{v+w'}}\\\cdot D\left(\phi'=\frac{\pi}{2}+\alpha,\phi=\frac{3\pi}{2},L=\left(v+w'\right)\right)\exp\left(-jk\left(v+w'\right)\right))\\+E'\left(1\right)\left[\exp\left(-jkw'\cos\alpha\right)+\frac{1}{\sqrt{w'}}\cdot D\left(\phi'=\frac{\pi}{2}+\alpha,\phi=\frac{3\pi}{2},L=w'\right)\exp\left(-jkw'\right)\right]\end{array}\right] \tag{23}$$

0.2λ (free space). A faster convergence can be obtained if an adaptative mesh strategy is applied, i.e. using a fine mesh around the corners of the corrugations, where stronger field intensities can be observed. To facilitate the comparison, the plot also presents the radiation patterns of an equivalent non-corrugated horn, calculated both using the EFIE technique outlined above (here, with 479 basis functions) and the UTD method by [14].

The results reveal good agreement between our proposed UTD-PO method and the EFIE technique for the horn with rectangular corrugations. Indeed, this agreement is particularly good for the main lobe and initial secondary lobes, which represent crucial parameters for the analysis of antenna radiation patterns.

Notably, because the radiation level is significantly lower at the back than at the front, the application of numerical techniques leads to increased divergence in line with the numerical parameters, e.g. mesh density, type of basis functions, and quadrature rule integration.

In computationally comparing the two methods presented in Fig. 2, we find that the UTD-PO calculations for the horn with rectangular corrugations need only 7 seconds to complete, while the results from the EFIE technique obtained using the same computer (an HP Z600 Workstation, 2.4 GHz Intel Xeon processor, 8 Gb of RAM) require 43 seconds, i.e. a six-fold increase. Thus, the proposed UTD-PO technique offers a significant improvement in computational efficiency compared to conventional techniques, such as EFIE, that segment the entire structure.

IV. CONCLUSION

A technique using a hybrid UTD-PO formulation was utilized to assess the E-plane radiation pattern of corrugated E-plane rectangular horn antennas that have rectangular corrugations. Validation of the technique was achieved by comparing it to the electric field integral equation (EFIE) solved using the method of moments (MoM). While there was good alignment between these approaches (particularly good for the main lobe and initial secondary lobes), the UTD-PO method demonstrated superior computational efficiency, providing the solution six times faster than EFIE.

REFERENCES

[1] R. E. Lawrie and L. Peters, "Modifications of horn antennas for low sidelobe levels," *IEEE Trans. Antennas Propag.*, vol. AP-14, no. 5, pp. 605–610, Sep. 1996.

[2] R. Baldwin and P. A. Mcinnes, "A rectangular corrugated feed horn," *IEEE Trans. Antennas Propag.*, vol. AP-23, no. 6, pp. 814–817, Nov. 1975.

[3] C. Mentzer and L. Peters, "Pattern analysis of corrugated horn antennas," *IEEE Trans. Antennas Propag.*, vol. AP-24, no. 3, pp. 304–309, May 1976.

[4] P. J. B. Clarricoats and A. D. Olver, *Corrugated Horns for Microwave Antennas*, London, U.K.: Peter Peregrinus, 1984.

[5] T. S. Bird, "Mode matching analysis of arrays of stepped rectangular horns and application to satellite antenna design," in *Proc. 7th Int. Conf. Antennas Propag., ICAP (IEE)*, vol. 2, Apr. 1991, pp. 849–852.

[6] A. Borgioli, R. Coccioli, G. Pelosi, and J. L. Volakis, "Electromagnetic scattering from a corrugated wedge," *IEEE Trans. Antennas Propag.*, vol. 45, no. 8, pp. 1265–1269, Aug. 1997.

[7] J. Teniente, R. Gonzalo, and C. Del-Rio, "Innovative high-gain corrugated horn antenna combining horizontal and vertical corrugations," *IEEE Antennas Wireless Propag. Lett.*, vol. 5, pp. 380–383, 2006.

[8] L. J. Foged, A. Giacomini, and R. Morbidini, "Dual-polarized corrugated horns for advanced measurement applications," *IEEE Antennas Propag. Mag.*, vol. 52, no. 6, pp. 199–204, Dec. 2010.

[9] L. Lucci, R. Nesti, G. Pelosi, and S. Selleri, "A stackable constant-width corrugated horn design for high-performance and low-cost feed arrays at millimeter wavelengths," *IEEE Antennas Wireless Propag. Lett.*, vol. 11, pp. 1162–1165, 2012.

[10] S. Manshari, S. Koziel, and L. Leifsson, "Compact dual-polarized corrugated horn antenna for satellite communications," *IEEE Trans. Antennas Propag.*, vol. 68, no. 7, pp. 5122–5129, Jul. 2020, doi: 10.1109/TAP.2020.2980337.

[11] A. F. Peterson, S. L. Ray, and R. Mittra, *Computational Methods for Electromagnetics*. Piscataway, NJ, USA: IEEE Press, 1998.

[12] M. Salazar-Palma, T. K. Sarkar, L.-E. García-Costillo, and R. Tanmoy, *Iterative and Self-Adaptive Finite-Elements in Electromagnetic Modeling*. Norwood, MA, USA: Artech House, 1991.

[13] W. L. Stutzman and G. A. Thiele, *Antenna Theory and Design*, 2nd ed. Hoboken, NJ, USA: Wiley, 1998, pp. 568–571.

[14] J.-V. Rodríguez, F. Quesada-Pereira, L. Juan-Llácer, E. Verdú-Rodríguez, J.-M. Molina-García-Pardo, and A. Álvarez-Melcón, "E-plane radiation pattern analysis of rectangular horn antennas with V-shaped corrugations by UTD-PO formulation," *Radio Sci.*, vol. 47, no. 3, Jun. 2012, Art. no. RS3011, doi: 10.1029/2011RS004926.

[15] J.-V. Rodríguez, F. Quesada-Pereira, L. Juan-Llácer, J.-M. Molina-Garcia-Pardo, and A. Álvarez-Melcón, "UTD-PO radiation pattern analysis of rectangular horn antennas with cylindrical corrugations," *IEEE Trans. Antennas Propag.*, vol. 62, no. 11, pp. 5911–5915, Nov. 2014, doi: 10.1109/TAP.2014.2355196.

[16] J. V. Rodriguez, J. M. Molina-Garcia-Pardo, and L. Juan-Llacer, "An improved solution expressed in terms of UTD coefficients for the multiple-building diffraction of plane waves," *IEEE Antennas Wireless Propag. Lett.*, vol. 4, pp. 16–19, 2005, doi: 10.1109/LAWP.2004.841624.

[17] J.-V. Rodriguez, M.-T.-M. Ingles, J.-M. Molina-Garcia-Pardo, L. Juan-Llacer, T. Fujii, and I. Rodriguez-Rodriguez, "UTD-PO formulation for the analysis of multiple-plateau diffraction when considering illumination from a low source," *IEEE Trans. Antennas Propag.*, vol. 69, no. 7, pp. 4241–4245, Jul. 2021, doi: 10.1109/TAP.2020.3044377.

[18] R. J. Luebbers, "A heuristic UTD slope diffraction coefficient for rough lossy wedges," *IEEE Trans. Antennas Propag.*, vol. 37, no. 2, pp. 206–211, Feb. 1989, doi: 10.1109/8.18707.

[19] R. G. Kouyoumjian and P. H. Pathak, "A uniform geometrical theory of diffraction for an edge in a perfectly conducting surface," *Proc. IEEE*, vol. 62, no. 11, pp. 1448–1461, Nov. 1974.

JOSÉ LORENTE-LÓPEZ was born in Murcia, Spain, in 2000. He received the degree in telecommunications systems engineering from the Universidad Politécnica de Cartagena (UPCT), Spain, in 2022. He is currently pursuing the M.Sc. degree in applied artificial intelligence with the Universidad Carlos III, Madrid, Spain. He is also working as a Researcher with the Universidad de Alcalá, Madrid, Spain. His research interests include the modeling of radio wave propagation in urban environments and machine learning applications.

JOSÉ-VíCTOR RODRíGUEZ was born in Murcia, Spain, in 1975. He received the degree in telecommunications engineering from the Universidad Politécnica de Valencia (UPV), Spain, in 2001, and the Ph.D. degree in communications engineering from the Universidad Politécnica de Cartagena (UPCT), Spain, in 2006. His Graduate thesis with the Lund Institute of Technology, Lund University, Sweden, in collaboration with Ericsson Mobile Communications AB. In 2002, he joined the Department of Information Technologies and Communications, UPCT, where he is currently a Full Professor. His research interest includes the modeling of radio-wave propagation in the mobile environment, with an emphasis on multiple-building diffraction.

FERNANDO QUESADA-PEREIRA (Member, IEEE) was born in Murcia, Spain, in 1974. He received the master's degree in telecommunications engineering from the Technical University of Valencia (UPV), Valencia, Spain, in 2000, and the Ph.D. degree from the Technical University of Cartagena (UPCT), Murcia, in 2007. In 1999, he joined the Radiocommunications Department, UPV, as a Research Assistant, where he was involved in the development of numerical methods for the analysis of anechoic chambers and tag antennas. In 2001, he joined the Communications and Information Technologies Department, UPCT, as a Research Assistant, and then as an Assistant Professor. In 2005, he was a Visiting Scientist with the University of Pavia, Pavia, Italy. In 2009, he was an invited Researcher with UPV. In 2011, he became an Associate Professor with UPCT. His current research interests include integral equation numerical methods for the analysis of antennas and microwave devices, along with microwave filters design and applications.

LEANDRO JUAN-LLÁCER (Senior Member, IEEE) was born in Albatera, Spain, in 1967. He received the B.S. degree in telecommunications engineering from the Universitat Politécnica de Catalunya, in 1993, and the Ph.D. degree in telecommunications engineering from the Universidad Politécnica de Valencia, in 1998. He is currently a Full Professor with the Department of Information Technologies and Communications, Universidad Politécnica de Cartagena, Spain. He has been participating in the COST actions 259, 273, 2100, and IRACON. His research interests include the characterization of radio wave propagation in mobile communication systems and the development of radio planning tools based on GIS.

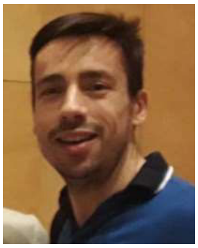

IGNACIO-RODRíGUEZ-RODRíGUEZ was born in Murcia, Spain, in 1980. He received the degree in technical industrial engineering and the degree in superior industrial engineering from the Universidad Politécnica de Cartagena (UPCT), Spain, in 2001 and 2004, respectively, and the Ph.D. degree in computer science with the Universidad de Murcia (UMU), Spain. In 2015, he joined the Department of Information and Communications Engineering, UMU. He is currently on a postdoctoral contract with the Telecommunications School, University of Malaga, Spain. His research interest includes the application of machine learning to biomedical signals, having works in other fields, such as radio wave diffraction.